Eur Biophys J (1985) 13: 37–44

European Biophysics Journal

Single-cell flux measurement by continuous fluorescence microphotolysis

M. Scholz[1], **K. Schulten**[2], **and R. Peters**[1]*

[1] Max-Planck-Institut für Biophysik, Kennedyallee 70, D-6000 Frankfurt/Main 70, Federal Republic of Germany
[2] Physik-Department, Technische Universität München, Theoretische Physik, D-8046 Garching, Federal Republic of Germany

Received December 28, 1984/Accepted May 16, 1985

Abstract. Continuous fluorescence microphotolysis (CFM) was adapted to flux measurements in single cells. The principle of the method is simple: Cells are equilibrated with a fluorescent solute, an individual cell is continuously irradiated by a laser beam focussed down to approximately the diameter of the cell, and fluorescence originating from the irradiated cell is monitored. In this procedure irradiation irreversibly photolyzes chromophores in the cell while fresh chromophores enter the cell by membrane transport (flux). The resulting fluorescence decay can be analyzed for the rate constants of both membrane transport and photolysis. As an experimental test of the new method the band-3 mediated transport of the fluorescent anion *N*-(7-nitrobenzofurazan-4-yl)-taurine (NBD-taurine) across the erythrocyte membrane was measured. For various experimental conditions good agreement between values obtained by CFM and by fluorescence microphotolysis (FM) was observed. By measurements on single ghosts it was furthermore found that photolysis of NBD-taurine is first-order with respect to the power of irradiation. On this basis a stepped-intensity procedure was worked out that facilitates data evaluation in flux measurements. Also, by analysing the relations between CFM and FM flux measurements a method was devised by which FM data can be corrected for (inevitable) photolysis.

Key words: Fluorescence microphotolysis, photobleaching, flux measurement, erythrocyte membrane, anion transport

Introduction

Cell function is based on various types of molecular transport. These processes occur under conditions of concentration, heterogeneity and topography not easily reconstituted in the test tube. It is therefore an important goal of molecular biology to characterize transport processes in situ, i.e. within the living cell. A method specifically developed for that purpose is fluorescence microphotolysis (FM). In recent years the method has been most frequently used to measure diffusion coefficients of proteins and lipids in cellular membranes although applications to artificial membranes were also numerous (for review see Ware 1984; Axelrod 1983; Peters 1981; Cherry 1979). The principle of FM is quite simple. A membrane protein, for instance, is labeled with a fluorescent chromophore. Under the microscope a small spot on the surface of an individual cell is illuminated by a focussed, highly attenuated laser beam and fluorescence is measured. By increasing the power of the laser beam by several orders of magnitude chromophores in the illuminated area are photolyzed and rendered non-fluorescent in a short time. Returning to the initial low beam power, fluorescence in the illuminated area is measured again. The time course of fluorescence indicates whether chromophores enter the photolyzed area from the surroundings and is used to derived transport coefficients.

After its introduction (Peters et al. 1974) FM was further developed (Edidin et al. 1976; Jacobson et al. 1976; Axelrod et al. 1976) and special versions were described (Smith and McConnel 1978; Koppel 1979; Thompson et al. 1981; Smith et al. 1981; Lanni and Ware 1982; Davoust et al. 1982). In addition, a concept was put forward which is referred to as Continuous Fluorescence Microphotolysis (CFM) (Peters et al. 1981; Brünger et al. 1985). In CFM, a spot on a fluorescently labeled cell surface is irradiated at constant, intermediate power (no intensity-step as in FM). Thus, photolysis and diffusion occur simultaneously. A theory was developed by which the experimental CFM data can be ana-

* To whom offprint requests should be sent

lyzed for the rate constants of both photolysis and diffusion. The theory is rather general because it also covers the FM-type experiment and can be applied to various patterns of irradiation in both space and time.

Recently, the FM method has been adopted to the measurement of membrane transport (flux) in single cells (Peters 1983, 1984a, b; Lang and Peters 1984; Peters and Passow 1984). After equilibration with a fluorescent solute the fluorescence of individual cells was measured. Then, solute was photolyzed in the cell interior by an intensive light pulse and transport from the medium into the cell followed by fluorescence measurements. This paper describes the adaptation of CFM to single-cell flux measurements. A theoretical framework was developed. CFM flux measurements were performed on a well defined system, namely anion transport by the band-3 protein of the erythrocyte membrane. The results were compared with those obtained in the same system by FM. Relations between CFM and FM were analyzed. As in diffusion measurements CFM is the more general case because both CFM and FM flux data can be analyzed by the same equations. It is also possible, for instance, to correct FM data for (inevitable) photolysis during fluorescence measurement.

Experimental

The FM apparatus used in this study is based on an instrument described previously (Peters and Richter 1981). However, several new components were added (Fig. 1). Among the new components are an image processing system (a photonic microscope system, model 1966-12, Hamamatsu) and a fast scanning stage (Zeiss). Fluorescence was measured by single-photon counting equipment (ORTEC) and evaluated by a MINC 11/23 computer (Digital Equipment). The ray path employed in flux measurements is indicated in Fig. 1 b. The 476.5 nm line of an argon laser was directed into the vertical illuminator of the microscope. In front of the vertical illuminator, at an image plane of the objective lens, a luminous-field diaphragm of 400 µm diameter was inserted into the laser beam. Using a 100-fold, n.a. 1.3, oil-immersion objective, the luminous-field diaphragm was imaged onto the stage object to give an irradiated are of 4 µm diameter. Fluorescence originating from the irradiated area was collected by the objective and projected onto a photometric attachment to the microscope. In the photometric attachment a photometric-field diaphragm was positioned such that it coincided with the image of the irradiated area. Fluorescence passing the photometric-field diaphragm was projected onto the cathode of a photomultiplier tube.

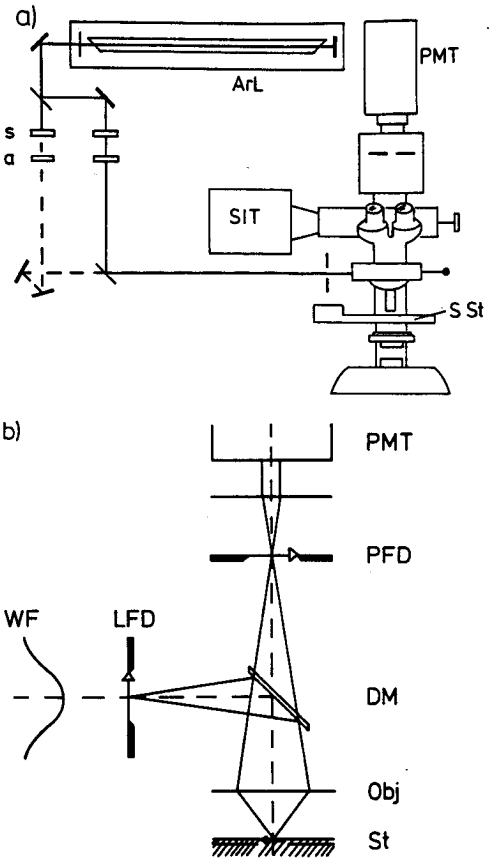

Fig. 1 a and b. The CFM apparatus. **a** A scheme of the set-up. *ArL*, argon laser; *s*, shutter; *a*, attenuator; *SIT*, image intensifying and processing TV system; *SSt*, scanning stage; *PMT*, photomultiplier tube. **b** A scheme of the ray path. *WF*, wave front of the laser beam; *LFD*, luminous-field diaphragm; *DM*, dichroic mirror; *Obj*, objective lense; *St*, stage object; *PFD*, photometric-field diaphragm; *PMT* photomultiplier tube

Methods used for preparing erythrocyte ghosts have been described previously (Peters and Passow 1984). Resealed human erythrocyte ghosts were suspended in a final medium consisting of 20 m*M* ethylene diaminotetraacetate, 130 m*M* sodium chloride and 1 m*M* of the fluorescent anion *N*-(7-nitrobenzofurazan-4-yl)-taurine (NBD-taurine). The ghost suspension was placed in a flat glass capillary (internal height 100 µm) and ghosts studied adhering to the upper glass-medium interface.

Theory

To model the CFM measurement we assume a cell of surface area S and volume V immersed in a large volume of medium. A fluorescent solute of concen-

tration in the medium $c_{out} = 1$ has reached an equilibrium concentration c_{in} in the cell. At time $t = 0$ a beam of constant light intensity and of an area which exceeds the cell's cross section is switched on. This induces a photoreaction which renders the irradiated solute partially non-fluorescent. The bleached solute inside the cell and in the extracellular medium is replenished by fresh solute through diffusion and through transport across the cell membrane. Both the intracellular and the extracellular diffusion is assumed to be much faster than the membrane transport (as discussed in Peters 1984a). Then the intracellular and extracellular concentration c and c_{out}, respectively, are spatially nearly constant. Since the extracellular medium is large one can assume that the photoreaction does affect the solute concentration only slightly, and one can safely assume $c_{out} = 1$ throughout the experiment. However, the intracellular concentration c should be time-dependent. Assuming that the photoreaction is first-order with rate constant k_p, and that the flux across the cell membrane is passive with rate constant k_t, one obtains for $c(t)$ the rate equation

$$\frac{dc}{dt} = -(k_p + k_t)\, c + k_t. \tag{1}$$

The solution of this equation is

$$\frac{c(t) - c(\infty)}{c(0) - c(\infty)} = e^{-Kt}, \tag{2}$$

where

$$K = k_p + k_t \tag{3}$$

and $c(0) = c_{in}$ and $c(\infty)$ are the initial and the final ($t \to \infty$) concentrations. For $c(\infty)$, the following relation holds

$$c(\infty) = k_t / K. \tag{4}$$

The measured total fluorescence, $F_t(t)$, is the sum of the time-dependent intracellular fluorescence, $F(t)$, and the time-independent extracellular fluorescence, F_{out}. F_{out} can be determined experimentally by complete photolysis of intracellular solute at the end of a CFM measurement. Assuming further that fluorescence is proportional to solute concentration it follows that

$$\frac{F(t) - F(\infty)}{F(0) - F(\infty)} = e^{-Kt} \tag{5}$$

where

$$F(\infty)/F(0) = k_t K. \tag{6}$$

The permeability coefficient, P, is given by

$$P = (V/S)\, k_t. \tag{7}$$

Results and discussion

The experimental basis of CFM flux measurements was visualized directly by TV imaging (Figure 2). Ghosts were immersed in an isotonic solution containing 1 m*M* NBD-taurine and placed in a capillary of 100 µm pathlength. Ghosts adhering to the upper glass-medium interface were imaged under phase-contrast conditions (Fig. 2a) and then irradiated by conventional light source (100 W high-pressure mercury lamp) employing a large luminous-field diaphragm. Fluorescence images were recorded immediately after onset of irradiation (Fig. 2b), after 10 s (Fig. 2c) and after 30 s (Fig. 2d). Ghosts in the irradiated area became progressively depleted of fluorescence whereas fluorescence in the medium changed little. This effect is also clearly shown by taking the difference of Fig. 2a and c, i.e. images stored in frame memory were subtracted from each other (Fig. 2e): background is almost completely cancelled whereas ghosts appear as bright spots. These experiments were performed at a temperature (22 °C) at which transport of NBD-taurine across the erythrocyte membrane is very slow (Peters and Passow 1984). The pictures therefore reflect the effects of the photochemical reaction and of solute diffusion in the medium but not of membrane transport. Nevertheless, the photographs suggest that CFM flux measurements could, in some cases, be performed with a conventional light source instead of a laser. In the CFM flux measurements described below the power of the laser beam delivered to the irradiated area was around 0.5 µW. That power can be provided by conventional light sources.

Figure 2 also illustrates a phenomenon known as optical sectioning (for review see Agard 1984): the optical components of the light microscope image only a thin layer around the focal plane whereas radiation from other planes of the specimen is rejected. If this were not the case then the fluorescence of the approximately 2 µm thick ghosts could not be discriminated against a background consisting of a 100 µm thick layer of fluorescent medium. A primary parameter in optical sectionining is the aperture angle of the objective lens. However, the luminour- and photometric-field diaphragms employed in flux measurements further reduce the depth of focus. What, then, is the thickness of the imaged layer? This question has been addressed previously by Koppel et al. (1976) and by Schneider and Webb (1981). However, since the actual layer thickness depends on instrument-specific parameters including geometric aberration of the objective lens we have measured layer thickness in our set-up. A closely packed monolayer of fluorescent latex beads

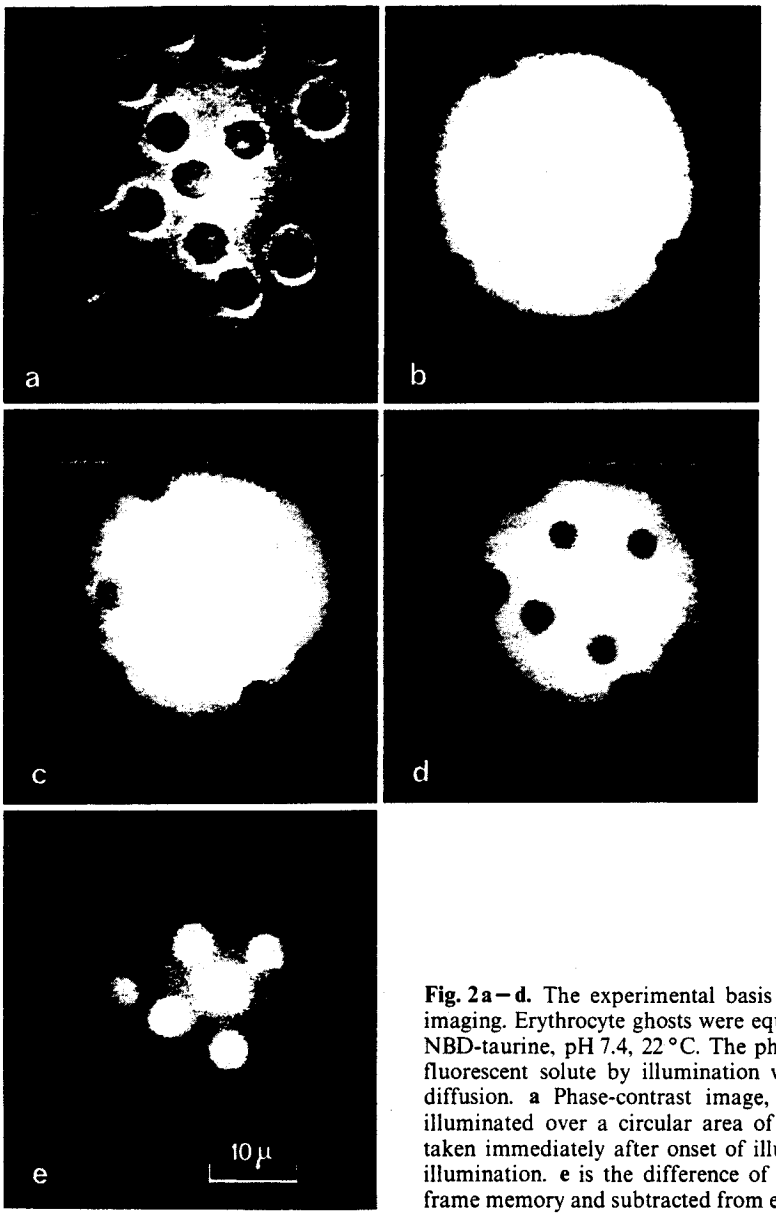

Fig. 2a–d. The experimental basis of CFM flux measurement demonstrated by TV imaging. Erythrocyte ghosts were equilibrated in an isotonic solution containing 1 m*M* NBD-taurine, pH 7.4, 22 °C. The photographs are to show that the cell is depleted of fluorescent solute by illumination whereas in solution solute is replenished by fast diffusion. **a** Phase-contrast image, **b–d** Fluorescence images of the same ghosts illuminated over a circular area of 30 µm by a high-pressure mercury lamp; **b** was taken immediately after onset of illumination, **c** was 10 s and **d** 30 s after continuous illumination. **e** is the difference of **b** and **d**, i.e. the digitized images were stored in frame memory and subtracted from each other

(diameter 0.9 µm) was prepared on a slide, covered with buffer and sealed with a cover slip. The specimen was placed on the stage of the microscope and fluorescence was recorded under exactly those conditions used in flux measurements, i.e. employing an irradiated area and an apparent photometric field of 4 µm diameter. The focal plane was determined visually and referred to as $z = 0$. The position of the layer on the optical (z-) axis was set by means of the stage micrometer and could be read with an accuracy of 0.5 µm. Results of a typical measurement are displayed in Fig. 3. The photomultiplier tube monitors only fluorescence from a layer a few µm thick. By placing an erythrocyte ghost in the intensity profile (see the scheme at the top of Fig. 3) it was estimated that about 70% of the total measured fluorescence derives from the interior of the ghost. This value agrees perfectly with the ratio of intracellular to total fluorescence obtained experimentally (Peters and Passow 1984; and this study). Figure 3 also reveals the experimental fluorescence profile to be slightly asymmetric with regard to the focal plane, an effect that was observed previously by Schneider and Webb (1981) and was attributed to geometric aberration of the objective lens. A theoretical intensity profile based on Eq. (7) of Koppel et al. (1976) is also plotted in Fig. 3. Although the equation was derived for the case of a

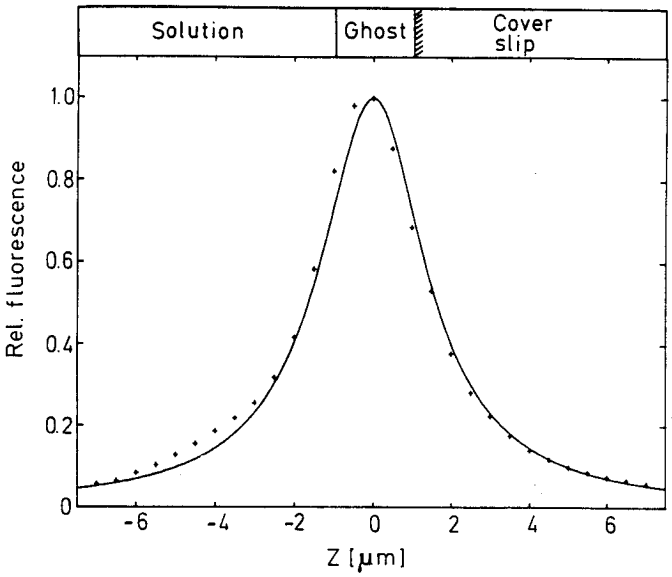

Fig. 3. Depth of focus in CFM flux measurements. A thin fluorescent layer was translated along the optical (z-) axis and fluorescence measured with the same set-up as in flux measurements. Crosses are experimental data. The full line was calculated according to an equation of Koppel et al. (1976) (see text). At the top the position of a ghost adhering to the glass-solution interface as in a flux measurement is indicated.

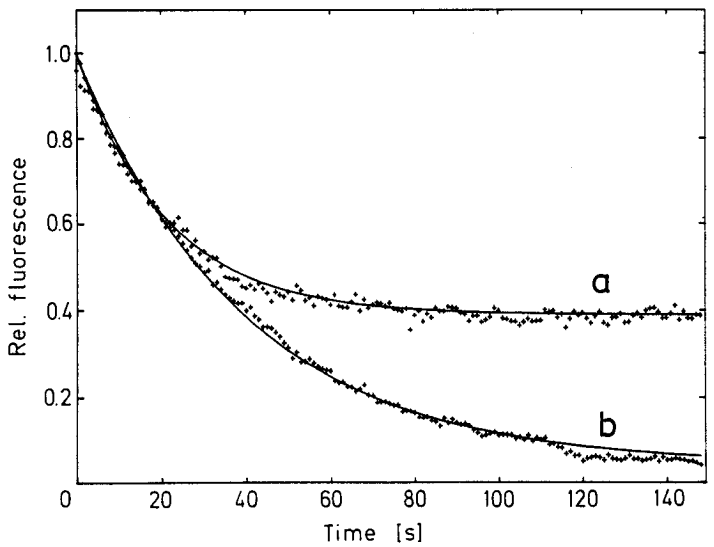

Fig. 4. CFM measurements of NBD-taurine flux across the erythrocyte membrane (pH 7.4, 46 °C). Normalized fluorescence, i.e. $F(t)/F(0)$, was plotted versus irradiation time. Curve a pertains to a normal, untreated ghost; curve b is of a ghost preincubated with 50 μM of the band-3 specific inhibitor DIDS. Crosses are experimental data, full lines are best fits according to Eq. (5)

Gaussian intensity profile of the irradiated area and furthermore is based on a number of approximations the fit with our experimental data is quite good. The theoretical profile was calculated for an aperture angle of 50.5° which is somewhat smaller than the actual aperture angle of the objective lens (n.a. = 1.3, oil). This may be attributed to the fact that the irradiating beam did not completely fill the objective aperture.

As an experimental test, CFM flux measurements were performed on resealed erythrocyte ghosts equilibrated in a solution of 130 mM sodium chloride, 20 mM ethylene diaminotetraacetate and 1 mM NBD-taurine. Eidelman and Cabantchik (1980) showed that transport of the fluorescent anion NBD-taurine across the erythrocyte membrane is specifically mediated by the band-3 protein. Recently NBD-taurine transport was measured in single ghosts (Peters and Passow 1984). Typical CFM flux measurements are shown in Fig. 4. The procedure for obtaining and evaluating data was the following. At first, the total fluorescence $F_t(t)$ was recorded as a function of irradiation time. When the fluorescence decay had reached equilibrium a laser flash of an energy sufficient to completely photolyze intracellular fluorescence was applied. Fluorescence immediately after the flash was assigned as background fluorescence F_{out}. The ratio $F_{out}/F_t(0)$ usually amounted to 0.3. Then, F_{out} was subtracted from F_t in order to obtain intracellular fluorescence, $F(t)$,

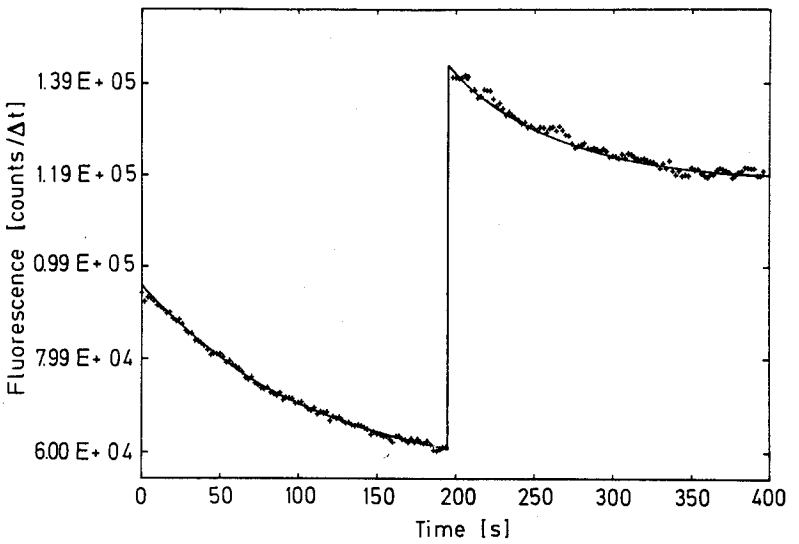

Fig. 5. A stepped-intensity CFM measurement of NBD flux across the erythrocyte membrane (pH 7.4, 40 °C). Fluorescence is plotted versus irradiation time. At $t = 196$ s the power of irradiation was suddenly increased by a factor of 2.25. From the fit the membrane rate constant can be calculated according to a simplified procedure (Eq. (8))

Table 1. Rate constants of NBD-taurine flux into resealed human erythrocyte ghosts. Comparison of CFM and FM measurements

	CFM[a]		FM[a]	
	k_t $10^{-4}\,s^{-1}$	n	k_t $10^{-4}\,s^{-1}$	n
46 °C, pH 7.4	150 ± 28	19	138 ± 23	16
46 °C, pH 7.4, 50 μM DIDS	15 ± 5	14	7 ± 5	5
40 °C, pH 7.0	91 ± 11	9	n.d.[b]	
40 °C, pH 7.4[c]	n.d.[b]		74 ± 23	120

[a] Mean ± SD of n measurements
[b] n.d., not determined
[c] Data from Peters and Passow (1984)

which was plotted in normalized form. A single-exponential function was fitted to the experimental data by a least-squares procedure yielding the rate constant K and the equilibrium value $F(\infty)$. The rate constant of membrane transport, k_t, was then calculated according to Eq. (6). Irrespective of the value of k_t the equilibrium level of fluorescence, $F(\infty)$, can be freely adjusted over the total possible range ($0.0 \leqq F(\infty)/F(0) \leqq 1.0$) because the power of irradiation and hence k_P can be varied over several orders of magnitude. However, in a given experiment k_t can be determined with optimum experimental accuracy if $k_p \cong k_t$ and $F(\infty)/F(0) \sim 0.5$. This condition was approximately fulfilled for curve a in Fig. 4 by employing approximately 0.5 μW of irradiation power. Curve a of Fig. 4 refers to NBD-taurine transport in a normal ghost at 46 °C; k_t was .0185 s^{-1}, whereas the rate constant of photolysis was $k_p = 0.0291\ s^{-1}$. Curve b refers to a ghost incubated in a 50 μM solution of the band-3 specific inhibitor 4,4′-diisothiocyanostilbene-2,2′-disulfonate (DIDS). In that case k_t was 0.0010 s^{-1} and k_p was 0.0245 s^{-1}. Results of several experimental series are given in Table 1. From a comparison with results obtained on the same system by FM it is apparent that both CFM and FM yielded the same values within an experimental accuracy of approximately ± 15%.

The methods described require knowledge of background fluorescence, F_{out}, in order to evaluate CFM flux data. F_{out} is dispensable, however, if a stepped-intensity procedure is employed. Consider a CFM flux measurement starting with a power P_1 of irradiation. When fluorescence has reached equilibrium the power is changed to P_2 and fluorescence recorded until a new fluorescence equilibrium has been established. Assuming that photolysis is first-order with respect to light intensity, i.e. $k_p \sim P$, and therefore $k_{p_2} = r^{-1} k_{p_1}$ where $r = P_1/P_2$, it follows that

$$k_t = (K_1 - r K_2)/(1 - r). \quad (8)$$

A stepped-intensity CFM flux measurement is shown in Fig. 5. Ghosts were equilibrated in an isotonic solution containing 1 mM NBD-taurine, pH 7.4, 40 °C. The power ratio was $r = 0.45$. Evaluation of the experimental data showed K_1 to be 0.0109 s^{-1} and K_2 to be 0.0157 s^{-1}. Using Eq. (8), k_t was calculated to be 0.0069 s^{-1}, i.e. in the range determined previously (Peters and Passow 1984).

Equation (8) assumes that photolysis is first-order with respect to intensity. Lanni and Ware (1981) described an elegant method for measuring the order of a photolysis reaction in free solution. The procedure involves the very same stepped-intensity procedure described above. It is carried out, however, in the absence of membrane transport. Then, the order n of the photolysis reaction can be

determined from the following equation (Eq. (7) of Lanni and Ware 1981):

$$\lim_{\Delta t \to 0} \frac{\ln \frac{\dot{F}(t_0 + \Delta t)}{\dot{F}(t_0 - \Delta t)}}{\ln r}, \tag{9}$$

where $\dot{F}(t_0 + \Delta t)$ and $\dot{F}(t_0 - \Delta t)$, respectively, are the fluorescence changes immediately before and after the intensity-step. We have used the procedure to measure the order of NBD-taurine photolysis in single ghosts by inhibiting membrane transport with 50 μM DIDS and subjecting ghosts to stepped-intensity measurements analogous to the one displayed in Fig. 5. Using Eq. (9) the reaction order was determined to be $n = 1.00 \pm 0.43$ (mean $\pm$ SD of 12 measurements).

The FM methods is based on certain idealizing assumptions. One of these assumptions is that during fluorescence measurements the degree of photolysis can be kept at a negligible level, i.e. that k_p is much smaller than k_t. Then, $K \cong k_t$ and eq. (5) holds also for FM-type experiments (see Peters 1983, 1984a). However, quite frequently in single-cell measurements the number of fluorophores is extremely small and the fluorescence signal is correspondingly poor. One then usually resorts to increasing the power of irradiation and may get into a regime where k_p can not be neglected. In that case the apparent rate constant $k_{t_{ap}}$ of the FM recovery curve is

$$k_{t_{ap}} = K = k_t + k_p. \tag{10}$$

In addition, an "immobile fraction" of the fluorophores is simulated because fluorescence does not recover to the level $F(-)$ before photolysis but only to the equilibrium level $F(\infty)/F(-) = k_t/K$. Therefore the apparent mobile fraction $R_{M_{ap}} = (F(\infty) - F(0))/(F(-) - F(0))$ is

$$R_{M_{ap}} = \left(\frac{k_t}{K} - \frac{F(0)}{F(-)}\right)\left(1 - \frac{F(0)}{F(-)}\right)^{-1}. \tag{11}$$

In the case where $F(0) = 0$ (i.e. complete photolysis of intracellular chromophores) Eq. (11) reduces to

$$R_{M_{ap}} = k_t/K. \tag{12}$$

Equation (12) provides a simple means by which FM flux data can be corrected for photolysis. An experimental example is given in Fig. 6. It refers again to a ghost in an isotonic solution with 1 mM NBD-taurine, pH 7.4, 46 °C. The apparent rate constant of recovery, $k_{t_{ap}}$, was 0.0276 s^{-1} and the apparent mobile fraction, $R_{M_{ap}}$, amounted to 0.62. Using Eq. (12) the true transport rate constant, k_t, was calculated to be 0.0171 s^{-1}.

In summary, this paper has described a new method for flux measurements in single cells. Due to a higher power of irradiation the fluorescence signal is considerably stronger in a CFM than in a FM measurement on the same specimen. Typically, signal strength may be 10- to 20-fold larger in CFM. This could be crucial when studying rare molecular species. Since CFM and FM are closely related it is possible to perform and evaluate experiments mixing principles of both techniques.

Acknowledgement. Support by the Deutsche Forschungsgemeinschaft (Pe 138/8-4) is greatfully acknowledged.

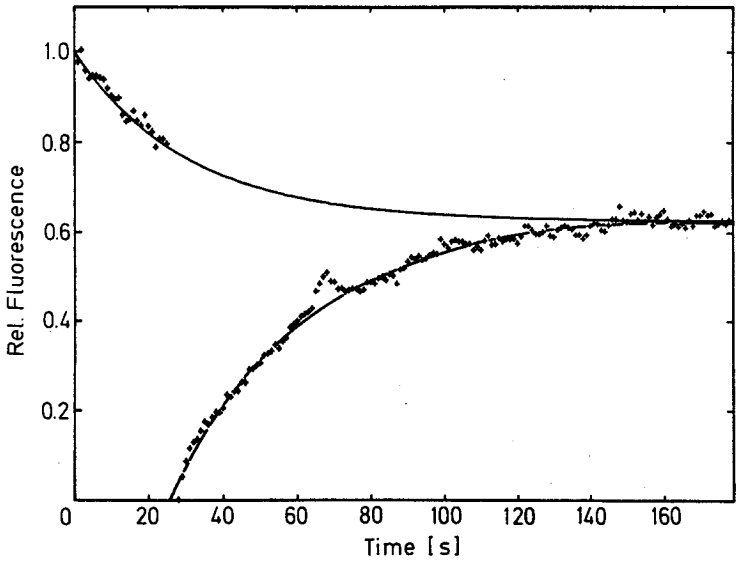

Fig. 6. A flux measurement in which the FM and CFM method were mixed. Normalized fluorescence is plotted versus irradiation time. Basically, the FM type was employed by 1) measuring fluorescence at low illumination power, 2) delivering a laser pulse to completely photolyze intracellular fluorescence, and 3) following solute influx by fluorescence measurement at the initial low illumination power. However, one of the idealizing assumption of the FM method – namely the absence of photolysis during measurement – was violated. This results in simulation of an "immobile fraction" and a wrong rate constant of membrane transport. The true rate constant of membrane transport can be derived using Eq. (11) and (12)

References

Agard DA (1984) Optical sectioning microscopy: Cellular architecture in three dimensions. Annu Rev Biophys Bioeng 13:191–219

Axelrod D (1983) Lateral motion of membrane proteins and biological function. J Membr Biol 75:1–10

Axelrod D, Koppel DE, Schlessinger J, Elson E, Webb WW (1976) Mobility measurements by analysis of fluorescence photobleaching recovery experiments. Biophys J 16:1055–1069

Brünger A, Peters R, Schulten K (1985) Continuous fluorescence microphotolysis to observe lateral diffusion in membranes. Theoretical methods and applications. J Chem Phys 82:7147–7161

Cherry RJ (1979) Rotational and lateral diffusion of membrane proteins. Biochim Biophys Acta 559:289–327

Davoust J, Devaux PF, Leger L (1982) Fringe pattern photobleaching, a new method for the measurement of transport coefficients of biological macromolecules. EMBO J 1:1233–1238

Edidin M, Zagyanski Y, Lardner TJ (1976) Measurement of membrane lateral diffusion in single cells. Science 191:466–468

Eidelman O, Cabantchik ZI (1980) A method for measuring anion transfer across red cell membranes by continuous monitoring of fluorescence. Anal Biochem 106:335–341

Jacobson K, Wu E, Poste G (1976) Measurement of the translational mobility of concanavalin A in glycerol-saline solutions and on the cell surface by fluorescence recovery after photobleaching. Biochim Biophys Acta 443:215–222

Koppel DE (1979) Fluorescence redistribution after photobleaching: a new multipont analysis of membrane translational dynamics. Biophys J 28:281–292

Koppel DE, Axelrod D, Schlessinger J, Elson EL, Webb WW (1976) Dynamics of fluorescence marker concentration as a probe of mobility. Biophys J 16:1315–1329

Lang I, Peters R, (1984) Nuclear envelope permeability: A sensitive indicator of pore complex integrity. In: Bolis CL, Helmreich EJM, Passow H (eds) Information and energy transduction in biological membranes. Alan R. Liss, New York, pp 377–386

Lanni F, Ware BR (1981) Intensity dependence of fluorophore photobleaching by a stepped-intensity slow-bleach experiment. Photochem Photobiol 34:279–281

Lanni F, Ware BR (1982) Modulation detection of fluorescence photobleaching recovery. Rev Sci Instrum 53:905–908

Peters R (1981) Translational diffusion in the plasma membrane of single cells as studied by fluorescence microphotolysis. Cell Biol Int Rep 5:733–760

Peters R (1983) Nuclear envelope permeability measured by fluorescence microphotolysis of single liver cell nuclei. J. Biol Chem 258:11427–11429

Peters R (1984a) Flux measurement in single cells by fluorescence microphotolysis. Eur Biophys J 11:43–50

Peters R (1984b) Nucleo-cytoplasmic flux and intracellular mobility in single hepatocytes measured by fluorescence microphotolysis. EMBO J 3:1831–1836

Peters R, Passow H (1984) Anion transport in single erythrocyte ghosts measured by fluorescence microphotolysis. Biochim Biophys Acta 777:334–338

Peters R, Richter HP (1981) Translational diffusion in the plasma membrane of sea urchin eggs. Dev Biol 86:285–293

Peters R, Peters J, Tews KH, Bähr W (1974) A microfluorimetric study of translational diffusion in erythrocyte membranes. Biochim Biophys Acta 367:282–294

Peters R, Brünger A, Schulten K (1981) Continuous fluorescence microphotolysis: A sensitive method for the study of translational diffusion in single cells. Proc Natl Acad Sci USA 78:962–966

Schneider MB, Webb WW (1981) Measurement of submicron laser beam radii. Appl Opt 20:1382–1388

Smith BA, McConnell HM (1978) Determination of molecular motion in membranes using periodic pattern photobleaching. Proc Natl Acad Sci USA 75:2759–2763

Smith LM, Weis RM, McConnel HM (1981) Measurement of rotational diffusion of membrane components by fluorescence photobleaching. Biophys J 36:73–91

Thompson NL, Burghardt TP, Axelrod D (1981) Measuring surface dynamics of biomolecules by total internal reflection fluorescence with photobleaching recovery or correlation spectroscopy. Biophys J 33:435–454

Ware BR (1984) Fluorescence photobleaching recovery. Am Lab (Boston) 16:16–28